

### Silicon-Based Structural Ceramics for the New Millennium

Edited by Manuel E. Brito Hua-Tay Lin Kevin Plucknett



# Silicon-Based Structural Ceramics for the New Millennium

#### Related titles published by The American Ceramic Society:

Advances in Joining of Ceramics (Ceramic Transactions, Volume 138)
Edited by Charles A. Lewinsohn, Mrityunjay Singh, and Ronald Loehman ©2003, ISBN 1-57498-153-6

Ceramic Armor Materials by Design (Ceramic Transactions, Volume 134) Edited by J. McCauley, A. Rajendran. W. Gooch, S. Bless, S. Wax, and A. Crowson ©2002, ISBN 1-57498-148-X

Advanced SiC/SiC Ceramic Composites - Developments and Applications to Energy Systems (Ceramic Transactions, Volume 144) Edited by A. Kohyama, M. Singh, H.T. Lin, and Y. Katoh ©2002, ISBN 1-57498-162-5

Innovative Processing and Synthesis of Ceramics, Glasses, and Composites VI (Ceramic Transactions Volume 135)

Edited by Narottam P. Bansal and J.P. Singh

©2002, ISBN 1-57498-150-1

Innovative Processing and Synthesis of Ceramics, Glasses, and Composites V (Ceramic Transactions Volume 129)

Edited by Narottam P. Bansal and J.P. Singh ©2002, ISBN 1-57498-137-4

Advances in Ceramic Matrix Composites VII (Ceramic Transactions Volume 128) Edited by Narottam P. Bansal, J.P. Singh, and H.-T. Lin ©2001, ISBN 1-57498-136-6

Advances in Ceramic Matrix Composites VI (Ceramic Transactions Volume 124) Edited by J.P. Singh, Narottam P. Bansal, and Ersan Ustundag ©2001, ISBN 1-57498-123-4

Innovative Processing and Synthesis of Ceramics, Glasses, and Composites IV (Ceramic Transactions Volume 115)

Edited by Narottam P. Bansal and J.P. Singh ©2000, ISBN 1-57498-111-0

Innovative Processing and Synthesis of Ceramics, Glasses, and Composites III (Ceramic Transactions Volume 108)

Edited by J.P. Singh, Narottam P. Bansal, and Koichi Niihara ©2000, ISBN 1-57498-095-5

For information on ordering titles published by The American Ceramic Society, or to request a publications catalog, please contact our Customer Service Department at:

Customer Service Department 735 Ceramic Place Westerville, OH 43081, USA

614-794-5890 (phone) 614-794-5892 (fax) customersrvc@acers.org (e-mail)

Visit our on-line book catalog at www.ceramics.org.





# Silicon-Based Structural Ceramics for the New Millennium

Proceedings of the Silicon-Based Structural Ceramics for the New Millennium symposium, held at the 104th Annual Meeting of The American Ceramic Society April 28—May 1, 2002, in St. Louis, Missouri.

#### Edited by

Manuel E. Brito

National Institute of Advanced Industrial Science and Technology

Hua-Tay Lin

Oak Ridge National Laboratory

Kevin Plucknett

Advanced Ceramics Group, QinetiQ

Published by

The American Ceramic Society 735 Ceramic Place Westerville, Ohio 43081 www.ceramics.org Proceedings of the Silicon-Based Structural Ceramics for the New Millennium symposium, held at the 104th Annual Meeting of The American Ceramic Society April 28—May 1, 2002, in St. Louis, Missouri.

Copyright 2003, The American Ceramic Society. All rights reserved.

Statements of fact and opinion are the responsibility of the authors alone and do not imply an opinion on the part of the officers, staff, or members of The American Ceramic Society. The American Ceramic Society assumes no responsibility for the statements and opinions advanced by the contributors to its publications or by the speakers at its programs. Registered names and trademarks, etc., used in this publication, even without specific indication thereof, are not to be considered unprotected by the law.

No part of this book may be reproduced, stored in a retrieval system, or transmitted in any form or by any means, electronic, mechanical, photocopying, microfilming, recording, or otherwise, without written permission from the publisher.

Authorization to photocopy for internal or personal use beyond the limits of Sections 107 and 108 of the U.S. Copyright Law is granted by the American Ceramic Society, ISSN 1040-1122 provided that the appropriate fee is paid directly to the Copyright Clearance Center, Inc., 222 Rosewood Drive, Danvers, MA 01923 USA, www.copyright.com. Prior to photocopying items for educational classroom use, please contact Copyright Clearance Center, Inc.

This consent does not extend to copying items for general distribution or for advertising or promotional purposes or to republishing items in whole or in part in any work in any format.

Please direct republication or special copying permission requests to the Senior Director, Publications, The American Ceramic Society, PO Box 6136, Westerville, Ohio 43086-6136, USA.

Cover photo: "Fracture surface of exposed Kyocera SN235 sample after flexural testing at 850°C and 0.003 MPa/s" is courtesy of H.T. Lin, T.P. Kirkland, and A.A. Wereszczak, and appears as figure 6(a) in their paper "Effect of Long-term Immersion Test on Mechanical Reliability of Candidate Silicon Nitride Ceramics for Diesel Engine Applications," which begins on page 261.

For information on ordering titles published by The American Ceramic Society, or to request a publications catalog, please call 614-794-5890.

4 3 2 1-06 05 04 03 ISSN 1042-1122 ISBN 1-57498-157-9



Prefacevii
Novel Synthesis and Processing
Colloidal Processing of Silicon Nitride
Viscoelastic Properties of Concentrated Silicon Nitride Slurries
Si <sub>3</sub> N <sub>4</sub> Powders Applied for Water-Based DCT
Synthesis of Si <sub>2</sub> N <sub>2</sub> O Ceramics from Desert Sand
Fabrication and Evaluation of Porous Ca-α SiAION Ceramics
Microstructures: Development and Characterization
High Resolution Imaging and Microanalysis of Silicon-Based Ceramics
Grain-Boundary Relaxation Process in Silicon-Based Ceramics Studied by Mechanical Spectroscopy
High Temperature Stiffness and Damping to Qualitatively Assess the Amorphous Intergranular Phase in Sintered Silicon Nitride and Carbide
High-Temperature Deformation of Silicon Nitride and its Composites

Improved Properties
SiAION Ceramics: Processing, Microstructure and Properties
Fracture Behavior of Porous Si <sub>3</sub> N <sub>4</sub> Ceramics with Random and Aligned Microstructure
Liquid Phase Sintering of SiC with AIN and Rare-Earth Oxide Additives
Effect of Additives on Microstructural Development and Mechanical Properties of Liquid-Phase-Sintered Silicon Carbide during Annealing
Corrosion of Silicon Nitride Materials in Acidic and Basic Solutions and under Hydrothermal conditions 213 M. Herrmann, J. Schilm, and G. Michael
Applications  Development of High-Temperature Heat Exchangers  Using SiC Microchannels
Characterization of Ceramic Components Exposed in Industrial Gas Turbines
Gelcasting SiAION Radomes
Effect of Long-Term Oil Immersion Test on Mechanical Reliability of Candidate Silicon Nitride Ceramics for Diesel Engine Applications
Index



The international symposium, Silicon-Based Structural Ceramics for the New Millennium: Recent Scientific and Technological Developments, was held during the 104th Annual Meeting of The American Ceramic Society (ACerS), April 28–May 1, 2002 in St. Louis, Missouri. This symposium focused on recent scientific and technological developments in silicon-based (i.e., silicon nitride, SiAIONs, silicon carbide, silicon oxynitride) structural ceramics. Attendees from academia and industry assessed the current state of the art and industrial case studies were advocated to highlight the development and application of these materials in real engineering environments. The symposium consisted of 55 contributions from 12 countries and five continents.

This volume of the Ceramic Transactions series contains selected papers on various aspects of synthesis and processing, characterization, properties and applications of silicon-based structural ceramics. The manuscripts were reviewed following The American Ceramic Society review process.

The editors wish to extend their gratitude to all the authors for their contributions and to all the participants and session chairs for their time and efforts. Thanks to all the reviewers for their useful comments and suggestions. Thanks are due to the staff of the Meetings and Publications Departments of ACerS for their tireless efforts. We especially appreciate the helpful assistance, cooperation and patience of Mary Cassells and Greg Geiger throughout the production process of this volume.

It is our hope that this volume will serve as a useful reference for scientist and engineers interested in the field of structural ceramics, and also will serve as a stimulus for continuing efforts in the implementation and wider use of silicon-based ceramics.

Manuel E. Brito Hua-Tay Lin Kevin Plucknett

### **Novel Synthesis and Processing**

#### COLLOIDAL PROCESSING OF SILICON NITRIDE

Eric Laarz, Anders Meurk and Lennart Bergström Institute for Surface Chemistry PO Box 5607 SE-11486 Stockholm Sweden

#### **ABSTRACT**

This review summarizes recent work related to the colloidal processing of silicon nitride. Silicon nitride surface chemistry, dissolution behavior, deagglomeration, dispersion and stabilization in aqueous medium are treated in detail, taking into account apparent interdependencies. Experimental results have been evaluated quantitatively and qualitatively to identify underlying mechanisms responsible for colloidal properties of silicon nitride powders. Fitting dissolution data at various pH and temperatures with suitable kinetic equations enabled us to determine the overall activation energy for dissolution and to identify different kinetic dissolution regimes. Evidently, the dissolution behavior of silicon nitride surface oxides and amorphous silica are very similar. It is further shown how milling conditions for the deagglomeration of silicon nitride powder containing hard particle agglomerates with inter-particle necks can be optimized. Forces between silicon nitride surfaces were measured with an atomic force microscope and evaluated using Lifshitz and DLVO theory and numerical data analysis. This approach allowed the verification of Hamaker constants for van der Waals interaction across various media as well as an assessment of charge regulation effects at varying pH and surface separation. By measuring forces between Si<sub>1</sub>N<sub>4</sub> surfaces with adsorbed polyacrylic acid dispersant, polymer-induced steric forces were shown to be very short-ranged. Hence, the dispersant's effect on colloidal stability is limited to a purely electrostatic contribution to the total particle interaction potential.

To the extent authorized under the laws of the United States of America, all copyright interests in this publication are the property of The American Ceramic Society. Any duplication, reproduction, or republication of this publication or any part thereof, without the express written consent of The American Ceramic Society or fee paid to the Copyright Clearance Center, is prohibited.

#### CONTENTS

#### INTRODUCTION

#### SURFACE CHEMISTRY AND POWDER DISSOLUTION

- Surface Chemistry
- Dissolution Behavior

#### DEAGGLOMERATION AND DISPERSION

#### INTERPARTICLE FORCES AND COLLOIDAL STABILITY

- van der Waals Forces
- Electrostatic Double Layer Forces and Charge Regulation
- Electrosteric Stabilization

**SUMMARY** 

**ACKNOWLEDGEMENTS** 

REFERENCES

#### INTRODUCTION

Present methods of manufacturing ceramic green bodies usually start with a suspension where the ceramic particles (powders, whiskers, platelets, etc.) are mixed with a liquid or a polymer melt, a proper dispersant, and possibly further additives (such as binders, plasticizers, and anti-foaming agents). Colloid science is frequently employed in order to remove heterogeneities and to optimize the suspension rheology [1, 2], e.g. by manipulation and control of the interparticle forces in powder suspensions [3, 4]. Hence, colloidal processing has become an integral part in the development and optimization of industrial processes for the production of technical ceramics.

This review describes some fundamental aspects of the colloid and surface chemistry of silicon nitride with importance for colloidal processing of aqueous suspensions. To support the understanding of the underlying colloidal concepts, we briefly introduce a background on the surface chemistry and powder dissolution. This is followed by a section on deagglomeration and dispersion. An orientation how the rheological properties of concentrated suspensions can be manipulated is also given.

#### SURFACE CHEMISTRY AND POWDER DISSOLUTION

The dissolution behavior of ceramic powders can play a crucial role in colloidal processing for several reasons. Changes of the elemental surface composition in the course of dissolution or dissolution/precipitation processes strongly affect the particle surface chemistry, which will modify interparticle forces and adsorption behavior of organic additives. Similarly, the release of ionic species due to dissolution increases the ionic strength in solution, which also alters the electrostatic interaction potential and adsorption processes. As further discussed in the following chapter, dissolution can even have a pronounced influence on agglomeration and deagglomeration processes.

Probably all ceramic materials used in technical applications dissolve to some extent when exposed to an aqueous environment. The dissolution rate, however, can vary by several orders of magnitude depending on the chemical composition and structure of the solid and the solution conditions. Hence, some ceramics are readily dissolved, while others exhibit a negligible dissolution rate. However, the dissolution rate is usually strongly temperature and pH dependent. Due to the large number of parameters that influence the dissolution, with many of them not directly accessible by experimental methods, there is a lack of comprehensive theories that can predict the dissolution behavior of ceramics in water. Consequently, it is common practice to describe the dissolution of a specific material in terms of experimentally determined dissolution rate constants.

In our discussion we place focus on the surface chemistry and dissolution kinetics of silicon nitride powder at alkaline pH. It will be shown that there is a strong interdependency of dissolution and surface chemistry, with a pronounced effect on colloidal stability and deagglomeration. After giving a brief account of earlier investigations on the surface chemistry of silicon nitride, thermodynamic and kinetic aspects of hydrolysis and dissolution in aqueous suspensions are addressed in detail. Experimental data for the dissolution kinetics at different temperatures and pH are presented and the overall activation energy for dissolution is determined. Additionally, similarities in the dissolution behavior of silicon nitride and silica are discussed.

#### Surface Chemistry

The surface chemistry of silicon nitride is well described by the dissociation and protonation reactions of amphoteric silanol (Si-OH) and basic secondary amine (Si<sub>2</sub>-NH) surface groups in water [5]

$$SiOH \leftarrow K_{AA} \rightarrow SiO^{-} + H^{+}$$
 (1 a)

$$SiOH \xrightarrow{+} \xrightarrow{K_{A2}} SiOH + H^{+}$$
 (1 b)

$$\operatorname{Si}_{2}NH_{2}^{+} \stackrel{K_{2}}{\longleftrightarrow} \operatorname{Si}_{2}NH + H^{+}$$
 (1 c)

where  $K_{AI}$ ,  $K_{A2}$  and  $K_B$  are equilibrium constants. The surface reactions and the surface densities of the two surface groups determine the pH-dependent surface charge density of silicon nitride and, thus, the isoelectric point, pH<sub>iep</sub> (i.e. the pH where the net surface charge is zero).

Based on Equation 1, Bergström and Bosted [5] derived an expression that relates the  $pH_{iep}$  to the relative amount of silanol,  $N_A$ , and secondary amine groups,  $N_B$ ,

$$\frac{N_{B}}{N_{A}} = \frac{-\left(\frac{10^{-pH_{up}}}{K_{A1}} - \frac{K_{A2}}{10^{-pH_{up}}}\right)}{\left(\frac{10^{-pH_{up}}}{K_{A1}} - \frac{K_{A2}}{10^{-pH_{up}}}\right)}}{\left(\frac{10^{-pH_{up}}}{K_{B}}\right)} \tag{2}$$

Relatively good agreement between  $N_B/N_A$  ratios calculated with Equation 2 and N/O-ratios obtained by XPS-measurements on powder surfaces was reported [5].

Earlier investigations have already demonstrated that the pH<sub>iep</sub> of Si<sub>3</sub>N<sub>4</sub> powders can vary dramatically depending on the powder synthesis process, powder treatment (thermal, chemical or mechanical), and wet processing conditions [5-15]. This has been attributed to differences in the oxygen content of the powder surface, which is mainly dictated by oxidation in air and hydrolysis reactions in water of the thermodynamically unstable Si<sub>3</sub>N<sub>4</sub>.

The oxidation of silicon nitride in air proceeds according to

$$Si_3N_4 + 3O_2 \xleftarrow{\kappa} 3SiO_2 + 2N_2 \tag{3}$$

when silica is assumed to be the main oxidation product. Investigations on pure Si<sub>3</sub>N<sub>4</sub>—films confirmed the presence of an amorphous, oxygen-rich surface layer with the oxygen concentration gradually increasing towards the surface [16]. The hydrolysis of silicon nitride in aqueous environments can be described with the overall reaction

$$Si_3N_4 + 6H_2O \stackrel{\kappa}{\longleftrightarrow} 3SiO_2 + 4NH_3$$
 (4)

assuming that silica is the main hydrolysis product. Similar reactions can be written when silicon oxynitride is the oxidation product. The silicon oxide

reaction product is present in the form of an amorphous surface layer, whereas the ammonia dissolves in water and protonates according to

$$NH_4^+ \stackrel{\kappa}{\longleftrightarrow} NH_1 + H^+ \tag{5}$$

#### Dissolution Behavior

The oxidized surface layer on silicon nitride is soluble in water and leaching studies have shown that not only oxidation and hydrolysis but also dissolution may significantly alter the surface composition and the associated surface charge [5, 12, 13]. The effect of oxidation and dissolution on the surface chemistry of silicon nitride is reflected in electrokinetic zeta-potential measurements and XPS-measurements on oxidized and leached powders as shown in Figure 1 and Table I. The leaching treatment consisted of dialyzing a dilute powder suspension against 0.01 M NaOH solution. An oxidation treatment of the as-received powder (UBE SN-E10, Ube Industries, Japan) shifted the pH<sub>iep</sub> to acidic values, whereas the leaching treatment caused a shift to basic values (Figure 1).

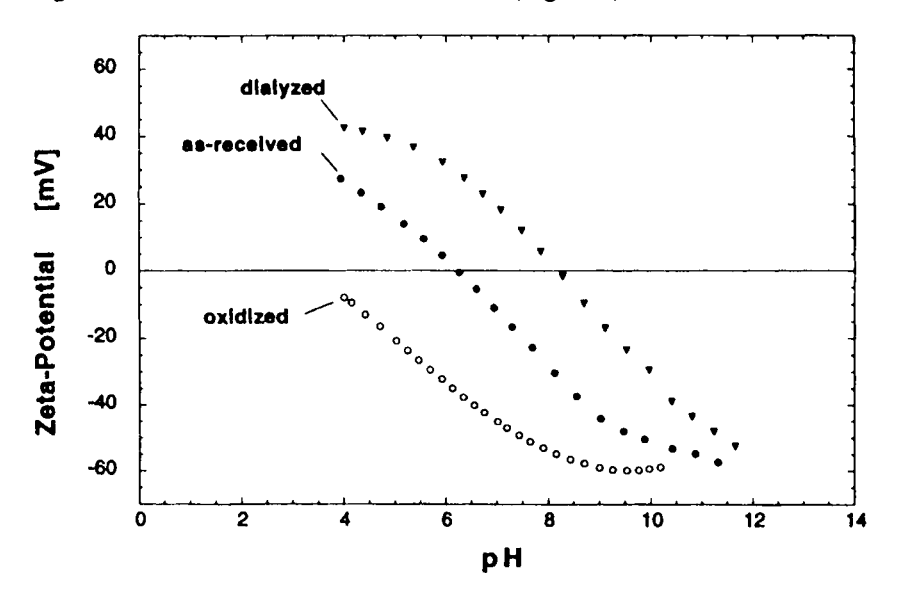


Figure 1: Zeta-potential of Si<sub>3</sub>N<sub>4</sub> suspensions with 5 vol% solids loading: as-received powder (●), after oxidation in air for 8 hours at 800 °C (O), and after dialyzing against 0.01 M NaOH for several days (▼). The counterion concentration was [Na+]=0.01 M in all experiments.

Both treatments lead to corresponding changes in elemental O/Si and N/Si ratios of the surface layer (Table I). These results agree with the suggested interdependency of the surface layer oxygen content, the relative amount of Si-OH and Si<sub>2</sub>-NH surface groups, and the surface charge density.

Table I. Results of XPS-measurements on as-received and modified silicon nitride powders used for the zeta-potential measurements shown in Figure 1.

Sample	N/Si	O/Si	N (1s) binding energy	Si (2p) binding energy
as-received	1.03	0.59	394.4 eV	99.0 eV
oxidized	0.85	0.80	394.6 eV	99.2 eV
dialyzed	1.33	0.19	397.7 eV	101.7 eV

The kinetics of silicon nitride dissolution was evaluated by studying the release of silicon as a function of time at varying pH and temperature (Figure 2). Except for the experiment conducted at pH=12, where NaOH was added, all dissolution experiments were performed without pH-adjustment. In these cases the release of ammonia (Equation 5) buffered the suspensions at pH=8.7±0.2. Figure 2 shows that the silicon nitride powder releases silicon quite readily and at pH=9 a saturation level is reached within days. Dissolution proceeds faster and a higher plateau value is reached at higher temperatures. At pH=12 dissolution is also very fast initially and slows down significantly after a while. However, the silicon concentration in solution continues to increase with time and no saturation plateau is reached.

For a completely dispersed suspension, the dissolution rate is expressed as

$$\frac{dc}{dt} = k_1 S - k_2 S c \tag{6}$$

where c(t) is the concentration of the solute,  $k_1$  the rate constant for dissolution,  $k_2$  the rate constant for deposition (reprecipitation) and S the available powder surface area in the suspension. At the particle concentrations used here (1-5 vol%), the release of silicon in aqueous suspensions of silicon nitride obeys the kinetic equation [17]

$$c(t) = c_s[1 - \exp(-kt)] \tag{7}$$

with  $c_s$  being the saturation concentration and k being the dissolution rate constant expressed in units of  $s^{-1}$ .

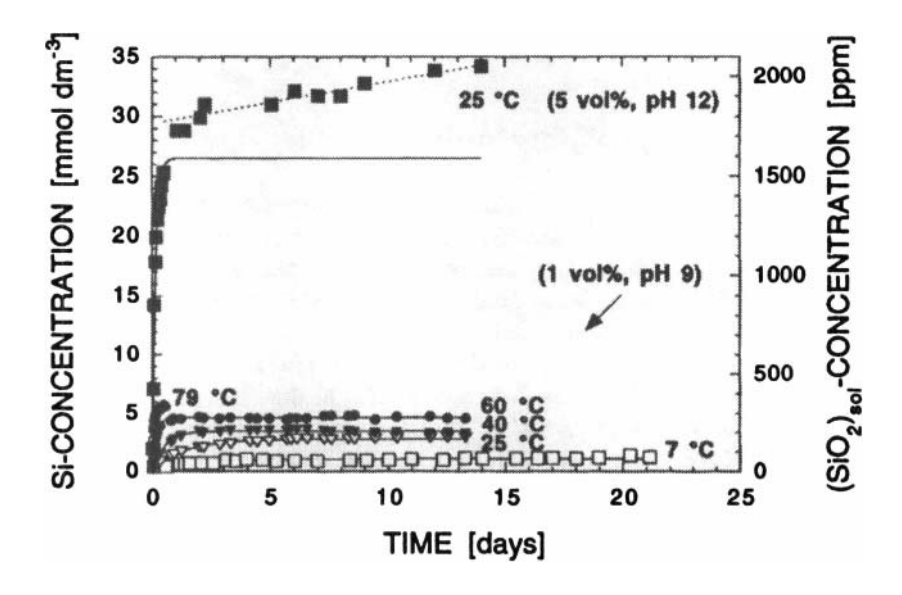


Figure 2: Kinetics of silicon release in dilute suspensions (1-5 vol%) of silicon nitride powder at pH=9 and pH=12. The experimental points are approximated by Equation 7 (solid lines). The dotted line is a least-square fit to the experimental data points. (from reference [18]]

The dependence of the dissolution rate constant, k, on temperature, T, can be described by an Arrhenius-type equation

$$k = k_0 \exp(-\frac{E^0}{RT}) \tag{8}$$

where  $k_0$  is the pre-exponential frequency factor,  $E^0$  the activation energy, and R the gas constant. By employing Equation 8 we can analyze the silicon release at pH=9 at various temperatures (Figure 2) in order to determine the overall dissolution activation energy. A least-square fit to the ln k vs. 1/T data yields  $k_0=9.8\times10^3$  s<sup>-1</sup> and  $E^0=51.7\pm0.1$  kJ mol<sup>-1</sup>. Apparently, the obtained activation energy for dissolution of oxidized silicon nitride is close to values reported for amorphous silica (70-80 kJ mol<sup>-1</sup>) [19]. Moreover, the experimentally determined amount of silicon dissolved from the oxidized silicon nitride surface at room temperature is around 170 ppm (Figure 2), which is also similar to reported values for amorphous silica,  $[SiO_2]_{sol}\approx100-150$  ppm at pH=3-9 [19]. Hence, from a dissolution point of view, the oxidized surface layer of silicon nitride behaves like

amorphous silica and it can be assumed that the surface oxide dissolves according to the overall reaction

$$SiO_2 + 2H_2O \leftrightarrow Si(OH)_4$$
 (9)

yielding colloidal silica Si(OH)<sub>4</sub> or other silicate species in solution [5, 17]. It is important to note that the solubility of silicon species increases dramatically at pH>10 [19]. As indicated by molecular orbital calculations, the formation of stable [Si(OH)<sup>5</sup>]<sup>-1</sup> complexes with a high solubility in water is a plausible explanation for this phenomenon [20].

The dissolution rate for oxidized silicon nitride is slightly higher than dissolution rates attributed by Segall et al [21] to the class of insulating covalent oxides (i.e.  $k<10^{-11}$  mol m<sup>-2</sup> s<sup>-1</sup>). This is most likely related to the amorphous structure of the surface layer; Iler, for example, reported that crystalline silica (\alphaquartz) dissolves slower than amorphous silica [19]. It has been suggested previously that the dissolution rate of insulating covalent oxides increases at alkaline pH, due to nucleophilic attack of water on metal-oxygen bonds [21]. Xiao and Lasaga described the pH-dependent hydrolysis of silica by means of ab initio quantum mechanical simulations [22, 23]. Their calculations suggest that the hydroxyl ion acts as a catalyst for the hydrolysis of siloxane bonds; hydrolysis via nucleophilic attack of water on Si-O-Si bridges is affected by the protonation state of the silanol surface groups. The activation energies for hydrolysis of silica are 121, 100, and 79 kJ mol<sup>-1</sup> for the cases where the respective surface silanols at the Si-O-Si bridge are neutral (Si-OH), protonated (Si-OH<sub>2</sub>), or deprotonated (Si-O ). It was further suggested that hydroxyl-catalyzed hydrolysis involves the formation of a transitional penta-coordinated Si-complex prior to the subsequent cleavage of the bridging siloxane bond. In fact, the hydrolysis of silica is controlled by the formation of the transitional complex. This step requires the highest activation energy of 79 kJ mol<sup>-1</sup>, the final rupture of the Si-O-Si bond involves an energy barrier of only 19 kJ mol<sup>-1</sup> [22, 23].

The above information allows a more detailed discussion of the peculiarities of silicon nitride dissolution at pH=12 and T=25 °C. Figure 2 shows that data points of the initial dissolution stage at this pH can be fitted with Equation 7. In contrast to the dissolution at pH=9, no saturation plateau is reached at longer times. Instead, one observes a slow dissolution characterized by a constant increase in concentration of dissolved silicon. The absence of a saturation plateau can be explained by the formation of penta-coordinated Si-complexes in solution and the corresponding increase in silicon solubility. The estimated dissolution rate constants for the initial and the later stage dissolution at pH=12 differ by three orders of magnitude, with the latter one being much lower than the dissolution

rate constant at pH=9 [24]. Hence, the rate determining step of the overall dissolution reaction in the constant-rate regime at pH=12 is not the same as in the initial stage of dissolution or in the dissolution experiments at pH=9.

An explanation for this behavior can be based on the data in Figure 3, where the time-dependent evolution of dissolved silicon concentration in solution is correlated to the change in surface composition expressed in terms of the O/Si atomic ratio. Apparently, the O/Si ratio reaches a constant value of 0.2 at about the same time as the constant-rate regime for the release of silicon begins. This correlation suggests that leaching reduces the thickness of the oxidized surface layer until a minimum thickness corresponding to O/Si=0.2 (Figure 3) and pH<sub>ieo</sub>=8.2 (Figure 1) is reached. At this point, a dynamic equilibrium is established where dissolution (Equation 9) can only proceed if new silica-like surface oxide is formed via hydrolysis of the Si<sub>1</sub>N<sub>4</sub> bulk phase (Equation 4). Hence, the experimentally observed transition at pH=12 from an initial regime with a high dissolution rate to a constant-rate regime with a very low dissolution rate is related to a change in rate-determining mechanisms. Apparently, the activation energy for hydrolysis of silicon nitride must be significantly higher than the activation energy for the dissolution of the amorphous surface oxide. This conclusion is also supported by quantum-chemical and ab-initio computations for hydrolysis of silicon nitride indicating that nucleophilic attack of water or hydroxyl ions leads to the formation of stable molecular complexes whose stability increases together with the degree of hydrolysis [25].

The experimental results presented here illustrate that the kinetics of silicon nitride surface oxide dissolution are controlled by two main factors, namely temperature and the activity of a nucleophilic agent (e.g. hydroxyl ions) catalyzing the hydrolysis reactions. The results further demonstrate that the extent of oxide removal through dissolution is determined by the saturation concentration of silicon species in solution and limited to the point where silicon oxide dissolution rate equals the rate of silicon nitride hydrolysis. Thus, providing sufficient silicon solubility by pH control can be used to minimize the surface oxygen concentration to a limit where O/Si=0.2 and pH<sub>iep</sub>=8.2. Alternatively, soxhlet extraction treatments [13] where the powder is continuously exposed to hot, fresh solution lead to the same result as indicated by results of Biscan et al [26, 27].

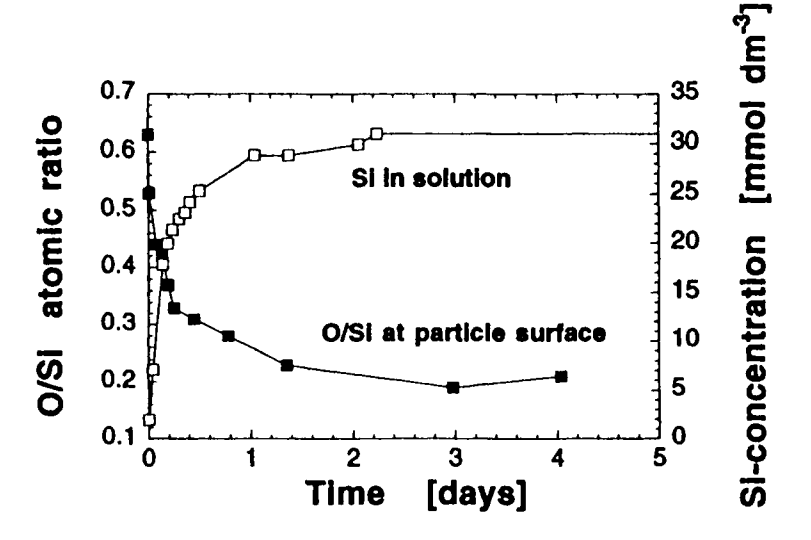


Figure 3: Si concentration in solution (□) and elemental O/Si ratio of the particle surface layer (■) obtained for a 5 vol% Si<sub>3</sub>N<sub>4</sub> suspension leached at pH=12 and T=25 °C (lines are meant to guide the eye).

#### **DEAGGLOMERATION AND DISPERSION**

Fine, sub-micronsized powders are always agglomerated in the dry, asreceived state. The dispersion process is strongly dependent on the strength of the interparticle bonds that keep the agglomerates together and the mechanisms that act to break the bonds. Removal or break-down of particle agglomerates is especially important considering the detrimental effect of such inhomogeneities on the mechanical properties of a sintered ceramic body. It is well known that both the size and number density of inhomogeneities play a crucial role in determining the strength and reliability of a ceramic material [3, 28].

The deagglomeration process in a moderately stirred dilute suspension of asreceived silicon nitride powder (UBE SN-E10, UBE Industries, Japan) is reflected by an evolution of the particle size distribution (PSD) with time (Figure 4). When comparing the size distribution obtained with a light scattering technique to electron microscopy results (Figure 5) it becomes evident that large agglomerates of primary particles are present in the suspension; the light scattering results indicate agglomerate sizes considerably larger than the size of the primary particles or crystallites. According to the transmission electron microscopy (TEM) investigations the size of the primary particles in the silicon nitride powder fall in the range of 50 to 200 nm, whereas the agglomerates in suspension have a size of up to 200  $\mu$ m. A primary particle size of 50 to 200 nm agrees well with 90 nm equivalent particle size derived from the measured specific surface area of 10.4 m<sup>2</sup> g<sup>-1</sup>.

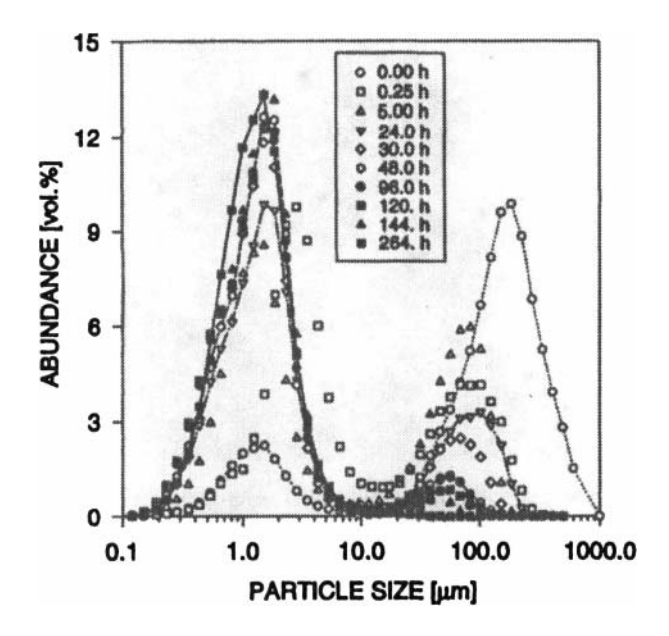


Figure 4: Evolution of particle size distribution with time in a mildly agitated 1 vol% Si<sub>3</sub>N<sub>4</sub> suspension at pH≈9 and 25 °C as measured by light scattering. The initial distribution (traced out by the dotted line) is characterized by a relatively large abundance of large agglomerates that disappear at long times in favor of smaller agglomerates. (from reference [25])

Figure 4 shows that large agglomerates, with sizes between 50 and 200  $\mu m$  are continuously broken down with time, and the population of smaller agglomerates (-1  $\mu m$  in size) is seen to increase. The two populations consist of agglomerates that are denoted as primary and secondary agglomerates in the following discussion. The absence of peaks at intermediate sizes in the PSD during deagglomeration suggests that primary agglomerates are eroded away from the large, secondary agglomerates (i.e. primary agglomerates constitute the



Figure 5: Bright-field TEM micrograph of the as-received silicon nitride powder showing crystallites at a high magnification (bar upper right corner=50 nm). (from reference [25])

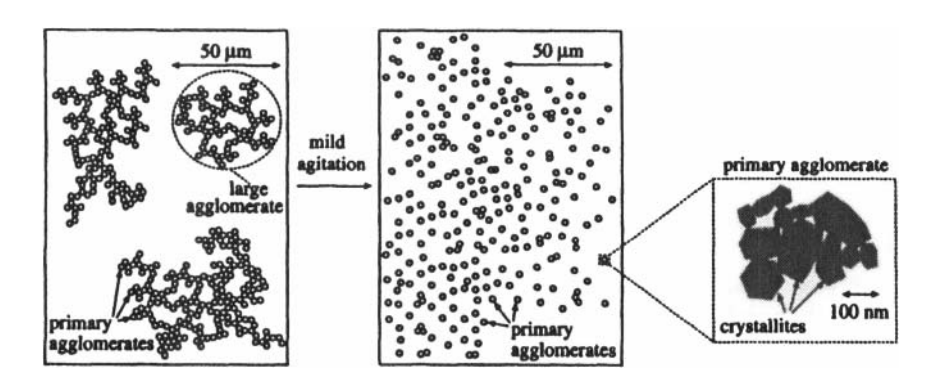


Figure 6: Schematic drawing illustrating the break-down of secondary agglomerates. (from reference [25])

building blocks of the secondary agglomerates). Hence, suspensions contain a hierarchy of agglomerates where the relative abundance of different size populations is constantly changing during the deagglomeration process. A conceptual view of this process is depicted in Figure 6.

Deagglomeration proceeds through the break-up of interparticle bonds in the aggregates when the applied force is larger than the adhesion force between aggregated particles. For a dilute suspension subjected to mild agitation, hydrodynamic drag is the dominating force on the aggregates. The magnitude of the drag force,  $F_d$ , exerted on a single particle of radius R in a flow field is approximately

$$F_d \approx 6\pi \upsilon \eta R \tag{10}$$

where  $\nu$  is the fluid velocity and  $\eta$  the fluid viscosity. The hydrodynamic drag force required to separate two particles is proportional to the interparticle adhesion force,  $F_{ad}$ 

$$F_d \approx \gamma F_{ad} \tag{11}$$

where  $\gamma$  is a numerical constant. As discussed previously by Desset [29],  $\gamma$  is close to unity when the drag force acts perpendicular to the surface and much smaller when the hydrodynamic force is parallel to the surface [29, 30]. Desset suggested  $\gamma$ =0.01-0.1 as a reasonable estimate for the detachment of small particles in a shear flow field [29].

For particles that are held together by attractive van der Waals forces, the adhesive interparticle force,  $F_{ad}$ , can be approximated with

$$F_{ad} \approx \frac{AR}{6D^2} \tag{12}$$

where A is the Hamaker constant and D the surface separation distance. This adhesive interparticle force is reduced by electrostatic repulsion at solution conditions where the surfaces carry a charge. The deagglomeration experiments were performed at pH $\approx$ 9 which is about 2.5 pH units above the isoelectric point of the silicon nitride powder (Figure 1). Therefore, it is expected that the net adhesive force between the silicon nitride particles is substantially smaller than Equation 12 predicts.

From Equations 11 and 12 one can obtain an estimate for the relative velocity between the particle and fluid phase required to separate two particles by hydrodynamic shear forces. Assuming that the maximum van der Waals attraction is reduced by one order of magnitude due to electrostatic repulsion between the charged surfaces and inserting the values  $\gamma=0.01$  [29],  $A=5\times10^{-20}$  J [31], and D=0.2 nm [3], one obtains  $v=10^{-2}$  m s<sup>-1</sup>. This value lies within the range of flow rates induced by moderate stirring,  $\sim 1-10$  mm s<sup>-1</sup>. Hence, it can be concluded that secondary agglomerates are held together by attractive van der Waals forces.

Apparently, the bonding forces between particles in primary agglomerates are much stronger than attractive surface forces, since primary agglomerates survive the stirring agitation (Figure 4) and even the ultrasonic treatment we used to prepare the electron microscopy samples. TEM studies revealed that agglomerates of 0.5-1 µm in size prevail in a suspension ultrasonicated at pH 10 (Figure 5).

The high strength of the primary agglomerates can be explained by the presence of rigid interparticle bridges, so-called necks. For example, measurements on boehmite [32] and silica [33] agglomerates with interparticle necks indicated agglomerate strengths of ≥20 MPa, values at least one order of magnitude higher than bond-strength estimates based on van der Waals forces only [32]. The interparticle necks in boehmite and silica were formed when the powder was dried, due to reprecipitation of dissolved species at particle contact points. Depending on the amount of dissolved material the size of the necks can be quite large (i.e. ranging from 10-100 nm).

In the case of sparingly soluble, synthetic non-oxide powders like silicon nitride, necks in the as-received powder may be formed during pyrolysis or calcination of precursor materials [3, 6] and/or through surface oxidation at particle contact points during storage. Therefore, the neck size should be on the same order as the thickness of the oxidized surface layer, i.e. approximately 1-10 nm [34-36].

A correlation between deagglomeration and dissolution is expected when interparticle necks consist of a soluble oxidic phase similar to that found on the particle surfaces. One expects that the neck size will be reduced by dissolution at a rate dictated by the dissolution kinetics. The effect of dissolution in alkaline medium on the neck size can be evaluated by using the experimentally determined dissolution rate constants. The decay of the neck radius with time, h(t), is related to the dissolution rate according to

$$h(t) \approx h - \frac{k_m t}{\rho}$$
with  $k_m \left[ g c m^{-2} s^{-1} \right] = 10^{-4} M_{SiN_{4/3}} k \left[ mol \ m^{-2} s^{-1} \right]$ 
(13)

where  $\rho$  is the density of the dissolved material and  $M_{SNAD} = 46.6 \text{ g mol}^{-1}$ .

Assuming a neck density of 2 g cm<sup>-3</sup> and using the experimentally determined k-values, one finds that the neck radius should decrease by 1 nm after approximately one week at 25 °C or after only three hours at 80 °C and pH=9. At pH=12 and 25 °C the same effect is obtained after 9 hours. Thus, the decay rate is strongly temperature and pH dependent. These estimates also show that silica based necks with a radius on the order of 1-10 nm can dissolve completely over reasonably short times when pH and/or temperature are increased.

The effect of dissolution on deagglomeration was evaluated experimentally by rheological measurements using the steady-shear response of concentrated silicon nitride suspensions prepared at solution conditions corresponding to varying dissolution kinetics (Figures 7 and 8). The untreated reference suspension with a volume fraction of 35% prepared at pH 9.4 in 0.01 M NaCl-solution is shown in Figure 7. It displays a weak shear thinning behavior, with the viscosity approaching a high-shear plateau value. Subjecting the powder to a 0.01 M NaOH solution results in a significant decrease in the viscosity. The pH of this suspension decreased rapidly during sample preparation, reaching pH 9.3 after about 30 min. The viscosity at high shear rates represents the hydrodynamic resistance to flow, which is mainly controlled by the efficiency of particle packing. Hence, the reduction in viscosity suggests that the alkaline conditions result in a rapid break-up of primary agglomerates, which releases immobilized liquid and allows improved particle packing.

An attempt to obtain an even lower viscosity by subjecting the powder to extensive leaching by keeping the suspension at pH 12 for two weeks was unsuccessful. The suspension displayed a strongly shear thinning behavior (Figure 7), typical of a flocculated suspension in which large flocs are broken down by the applied shear. The flocculation was induced by the high ionic strength in this system. High counterion-concentrations, approximately 50 mM Na<sup>†</sup>, were obtained because NaOH had to be continuously added to maintain the pH at 12. This effect is caused by the ionization of silicic acid at high pH. Since the silicic acid in solution is produced through powder dissolution, the amount of sodium hydroxide needed to keep a constant pH should be directly proportional to the amount of dissolved material.

In contrast, if the excess Na<sup>+</sup> and silicic acid are removed by dialysis, the degree of shear thinning and the viscosity are substantially reduced. The dialyzed suspension displays a nearly Newtonian shear behavior at 34 vol% with a high-shear viscosity comparable to a suspension viscosity at only 20 vol% measured directly after mixing. Similar results are obtained at 43 vol% solids loading (Figure 8). Hence, strong leaching leads to deagglomerated and low-viscous suspensions even at very high particle concentrations, but flocculation occurs if

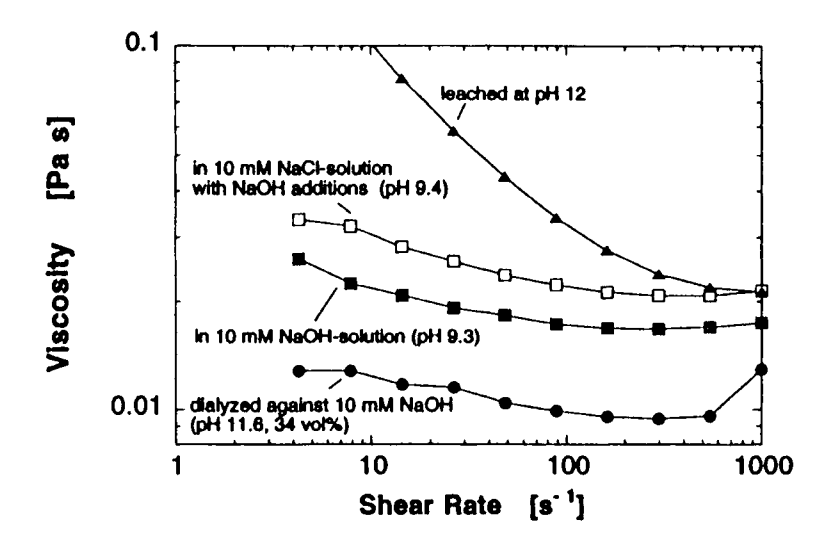


Figure 7: The steady-shear viscosity of 35 vol% suspensions at pH≈9.5 and pH≈12. (from reference [18])

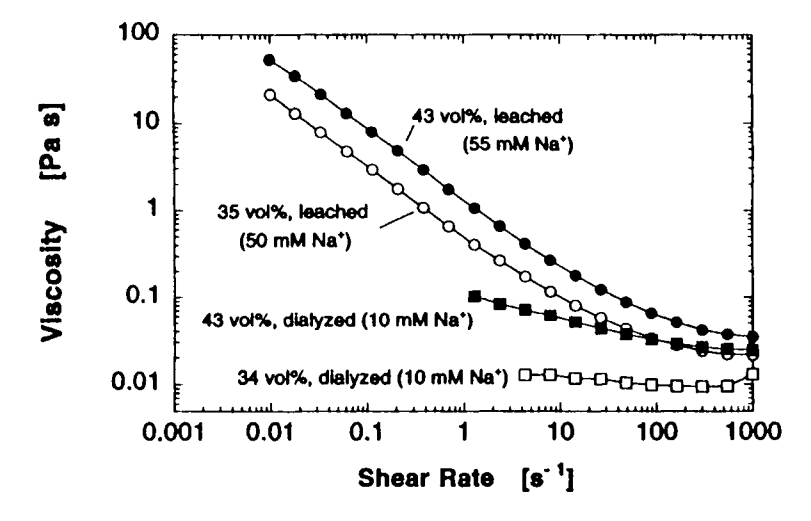


Figure 8: The steady-shear viscosity of 35 and 43 vol% suspensions at pH~12. The approximate counter-ion concentration in solution is given in parenthesis. (from reference [18])

the corresponding increase in counterion concentration is allowed to exceed the critical flocculation concentration of the system.

#### INTERPARTICLE FORCES AND COLLOIDAL STABILITY

Once a deagglomerated powder is dispersed in a liquid, repulsive interparticle forces of sufficient range and magnitude are necessary to maintain colloidal stability over extended periods of time. The dominating interparticle forces in colloidal ceramic suspensions are usually van der Waals forces and electric double layer forces. The van der Waals forces are always attractive in aqueous suspensions. Double layer forces are repulsive in simple one-component systems, but may become attractive in multi-component systems. Magnitudes of both the van der Waals and the electric double layer forces are strong functions of surface separation and, for the latter, also strongly dependent on pH and ionic strength.

The force-distance relationship for particle interactions can be calculated or obtained experimentally, e.g. with atomic force microscopy. We used a colloidal-probe technique to measure forces between silicon nitride surfaces. A silicon nitride tip or a nitrided silica sphere attached to the tip of a cantilever was moved towards a flat silicon nitride wafer surface and the deflection of the cantilever due to interaction forces was recorded as a function of surface separation [37-39]. Knowing the cantilever spring constant and the diameter of the sphere, the interaction potential per unit area, W(D), can be calculated by using the Derjaguin approximation

$$W(D) = \frac{F(D)}{2\pi R} \tag{14}$$

where D is the surface separation and R the probe radius. Information about the nature of the interaction forces was obtained by comparing the measurement data quantitatively with theory. Rheology combined with zeta-potential measurements provide another powerful, albeit more indirect, approach to describe the effect of dispersants on colloidal stability in ceramic suspensions. The attractive or repulsive nature of the total interaction force is reflected by suspension viscosity and shear thinning behavior. Zeta-potential measurements can help to assess double-layer force contributions to the total interaction potential. Ideally, all three techniques may be combined to link the macroscopic suspension properties to interaction forces.

#### van der Waals Forces

All ceramic powders experience van der Waals forces. This force is electrodynamic in origin as it arises from the interactions between oscillating or rotating dipoles within the interacting media. The van der Waals interaction free